

Introducing the Carpal-Claw: a Mechanism to Enhance High-Obstacle Negotiation for Quadruped Robots

Victor Barasuol¹, Sinan Emre¹, Vivian Suzano Medeiros^{1,2}, Angelo Bratta¹, and Claudio Semini¹.

Abstract—The capability of a quadruped robot to negotiate obstacles is tightly connected to its leg workspace and joint torque limits. When facing terrain where the height of obstacles is close to the leg length, the locomotion robustness and safety are reduced since more dynamic motions are required to traverse it. In this paper, we introduce a new mechanism called the Carpal-Claw, which enables quadruped robots to negotiate higher obstacles and adds safety to the locomotion by allowing the robot to negotiate obstacles under static and quasi-static locomotion and regular joint torque demands. The design of the mechanism is detailed, as well as the methodology to exploit the mechanism in the locomotion control framework. The Carpal-Claw functionality is validated through various experiments on a very high obstacle and stairs-like terrains using an Aliengo robot. We demonstrate how Aliengo can safely descend a step height of 40cm, which is 80% of its leg length. To the best knowledge of the authors, this is the first time a mechanism like the C-Claw is proposed for improving quadruped robot locomotion over high obstacles.

I. INTRODUCTION

Recent works in legged locomotion have focused on the development of planning and control systems that allow navigation in highly unstructured environments that include climbing and descending high obstacles. Such capability can be helpful for legged robots in a number of scenarios, especially in areas of natural disasters or collapsed terrain. Although advances in robotic technology have led to the development of robots capable of successfully navigating stairs, the negotiation of high obstacles relative to robot size remains a challenge and often requires specific strategies to be executed safely.

Boston Dynamics [1] has gained significant attention for their quadruped robot Spot, mainly due to its elegant stair-climbing capabilities, showcased in various videos. However, during stair descents, Spot is required to orient its nose upwards to reduce the risk of falling. Furthermore, the literature has recently documented that several quadruped robots, such as ANYmal [2], Aliengo [3], Cheetah-3 [4] or HyQReal [5], have demonstrated proficient stair-climbing capabilities. Their climbing and descending abilities on stairs differ due to their leg structures [6]. For instance, ANYmal

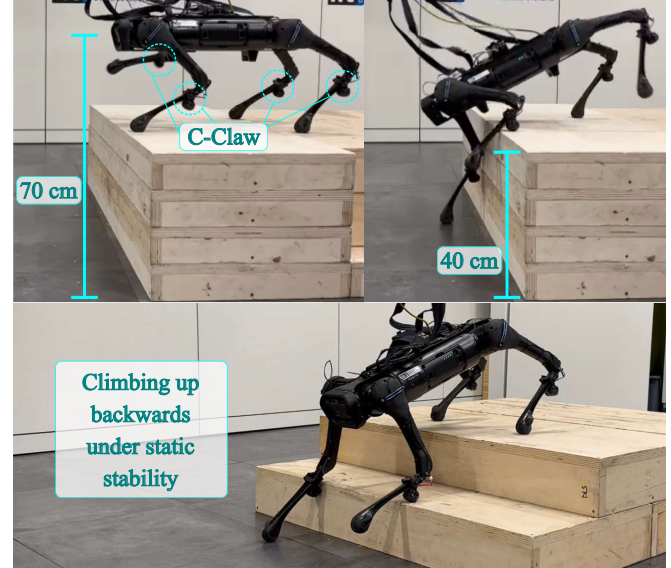


Fig. 1. Aliengo robot descending an obstacle of 40 cm height, in one of the experimental scenarios, using the proposed C-Claw mechanisms. The initial height of the robot w.r.t. the floor is about 70 cm, and the maximum robot leg length is about 50 cm.

has an inward-pointing configuration for its legs so it can descend stairs by orienting its nose down [7].

However, while quadruped robots have shown promise in the field, numerous challenges and concerns still limit their widespread adoption for safe applications, particularly when it comes to stair-descending tasks. Safety is of paramount concern when deploying quadruped robots, especially for descending stairs. Researchers have approached the stair-climbing problem from various perspectives, with motion planning emerging as a key strategy. Fankhauser et al. [8] presented a perceptive rough terrain locomotion that leverages a pre-acquired terrain map to assist a robot's motion planning for stair climbing or other complex terrains. In [9], authors introduced an optimized static gait for quadruped robots to navigate stairs. Their approach studied achieving stable poses on stairs and then employed a high-level planner to enhance stair-climbing capabilities by adjusting step lengths.

Liang et al. [10] proposed an algorithm for stable adaptive stair climbing by quadruped robots, utilizing vision-based depth camera data for terrain and geometry understanding. The primary goal of the algorithm is to allow quadruped robots to climb stairs in complex environments while maintaining stability and adaptability. The algorithm leverages

¹ Dynamic Legged Systems (DLS) lab, Istituto Italiano di Tecnologia (IIT), Genova (Italy). E-mail: name.surname@iit.it. Research partially funded by the European Union - NextGenerationEU and by the Ministry of University and Research (MUR), National Recovery and Resilience Plan (NRRP), Mission 4, Component 2, Investment 1.5, project “RAISE - Robotics and AI for Socio-economic Empowerment” (ECS00000035)

² Mechanical Engineering Department, University of São Paulo (EESC/USP), São Paulo, Brazil. Research partially funded by FAPESP, process number 2023/00249-0.

a depth camera to capture information about the terrain and geometry of the stairs. Another study [11] focuses on autonomous stair climbing with perception, combining perception, geometric information extraction, foothold planning, and model predictive control. Their framework aims to enable quadrupedal robots to navigate staircases autonomously. However, these approaches focused only on perception and stability on stairs and obstacles. Either they need a vision-based system to see the map, or the parameters of the stairs need to be defined beforehand.

Legged locomotion in highly unstructured environments has been addressed with reinforcement learning in recent studies [12]. Lee et al. [13] present a motion controller for blind legged locomotion in challenging natural environments. The controller is driven by a trained policy that acts based only on proprioceptive measurements from joint sensors and an IMU. Agarwal et al. [14] present a locomotion system capable of handling stairs, gaps, and stepping stones. Their approach uses depth information from an onboard camera as input to a policy trained to estimate terrain information that conditions a base feedforward walking policy. The results show the Unitree A1 robot navigating in scenarios with large obstacles relative to its size.

A recent study conducted by researchers from ETH Zurich [15] presents a detailed investigation into reinforcement learning, addressing various scenarios, including the challenging task of climbing stairs and high obstacles. In their methodology, they focused on training advanced locomotion skills for quadruped robots. These acquired skills were adapted and selected based on the specific terrain conditions encountered during locomotion. Furthermore, an integral aspect of their approach involved training a perception module, which was dedicated to reconstructing environmental obstacles from potentially noisy sensory data. The practical implementation of their research involved real-world experiments, wherein they employed the ANYmal-D robot. These experiments showcased the robot's capabilities in both climbing and descending, even when confronted with substantial height differences in the terrain.

Another approach for high obstacle negotiation for quadruped robots is using jumping motions [16]. In [17], a trajectory optimization algorithm is used to allow the MIT-Cheetah 3 to jump up and down a desk with a height of 76 cm. The motion planner is coupled with a landing controller designed for stabilizing the robot's position and orientation after impact. Similar jumping motions have been shown for the ANYmal robot using end-to-end reinforcement learning [18]. A jump over a 40 cm obstacle during a running motion is demonstrated for the MIT-Cheetah 2 using a model predictive approach that chooses the optimal position to initiate the jump prior to the obstacle [19]. In this case, obstacle negotiation is performed at a higher speed, and the goal is not to climb the obstacle, but to jump over it. Multi-contact motion planning has been employed for high obstacle negotiation by a humanoid robot in [20]. Their approach exploits the robot's upper limbs to provide additional support for the climbing maneuver. The trajectory

is optimized using data collected from human demonstrations as an initial solution. In general, such acrobatic motions impose strong requirements on joint torques and are not particularly suitable for applications in which safety is a major concern.

In this paper, we introduce a novel mechanical structure called the *Carpal-Claw*, or simply *C-Claw*. Its major goal is to enhance the quadruped robot locomotion on stairs and during high-obstacle descending. It allows the robot to better make contact with the obstacles and increase the motion controllability. While prior literature has predominantly focused on algorithmic solutions for stair climbing, we recognize the significance of enhancing a robot's physical capabilities. The C-Claw incorporates a specialized mechanism for detecting the ground as it engages, thereby contributing to a safer and more effective object negotiation.

The main contributions of this work are:

- A new mechanical structure called the C-Claw, is primarily designed to serve as an additional contact point for enhancing robot locomotion capabilities. Additionally, this innovative feature enables the robot to sense and gather contact information while descending high obstacles and walking on stairs. To the best knowledge of the authors, this is the first time such a mechanical structure has been employed in this context;
- Our approach increases foothold options during stair descent, which leads to facilitating climbing-down maneuvers from elevated positions. The additional contacts provided by the C-Claw reduce the effective height of the obstacles and are used by the locomotion framework to perform safer and controlled descending motions;
- The C-Claw is validated with extensive experimental tests with the Aliengo robot walking on a stair-case scenario and climbing down a 40 cm high step, which represents 80% of the maximum leg length.

This paper is organized as follows: Section II explains the inspiration and concepts behind the mechanism and its design. In Section III we describe how the C-Claw contact feedback can be exploited in a control framework to enhance locomotion capabilities. Experimental results, validating the proposed mechanism and control feedback, are presented in Section IV. Section V closes the paper with conclusions and directions for future work.

II. C-CLAW MECHANISM

This section introduces the concepts behind the C-Claw mechanism and provides an overview of its mechanical design and hardware functionality.

A. Inspiration and Concept Behind the Mechanism

The C-Claw gets inspiration from two biological mechanisms found on quadrupeds: the *Carpal Pad* and the *Claw*. The carpal pad of dogs, for example, has the main functionality of sensing contact interactions during fast locomotion (to generate the animal's movements), and giving additional traction to stop or when descending high inclines [21]. The claw mechanism, in turn, for what regards locomotion, helps

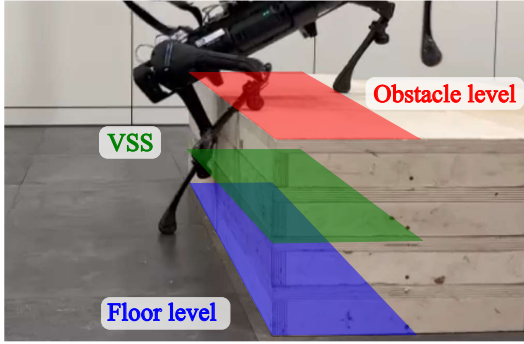


Fig. 2. Support surfaces during obstacle descending: in red and blue, the real obstacle and floor surfaces, respectively; in green, the Virtual Support Surface (VSS) that reduces the effective height of the obstacle.

the animal in increasing the range of forces that can be applied during contact interaction. If recalling the concept of a surface friction cone, one can see that the deployment of a claw leads to an increase in the friction coefficient, up to the extreme level of being able to pull on a surface and not only push. The proposed C-Claw mechanism, depicted in Fig. 3, combines some of the advantages of both biological mechanisms: first, it is used to detect an unusual contact interaction with the environment; second, it can tell about the shape of the contact surface underneath the leg; and third, it can be used to engage the robot's lower-leg onto the surface, allowing to produce a broader range of forces to control the locomotion. All these elements can be exploited to increase the robot's capabilities, enhancing the locomotion robustness and safety on stairs or stair-like shapes.

To give a perspective on how the C-Claw increases the robot's capabilities in going down high obstacles, we introduce the concept of *Virtual Support Surface* (VSS). The VSS is an intermediate surface between the obstacle level (from where the robot starts) and the floor level created by the C-Claw engagement with the obstacle, that reduces the effective distance between supporting surfaces during the descending motion. The position of the VSS depends on the distance between the foot and C-Claw and the robot's lower-leg angle with respect to the obstacle surface. Figure 2 illustrates the concept of the VSS.

B. Mechanical Design of the C-Claw

The C-Claw can be used to upgrade existing or newly designed quadruped robots by clamping it to the shin. In theory, if the robot is closer to the ground, it will have more reachable contacts on the ground. Therefore, this concept is followed and the C-Claw is positioned on the shin as close as possible to the knee joint. Figure 3 shows the exact location of the C-Claw in the CAD environment. Also, a clamp mechanism is designed by using the specific geometry of the robot's shin. With this mechanism, the C-Claw was constrained in three directions to the leg.

Figure 3 also shows a cross-section of the C-Claw with a description of its key elements. Part-B is the main body of the C-Claw which consists of the electrical elements to

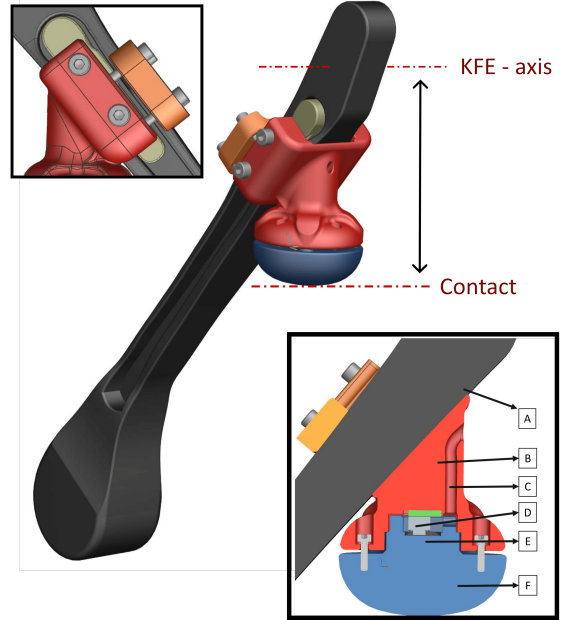


Fig. 3. Computer-aided design (CAD) model of the C-Claw. As seen in the side view, the C-Claw is fully constrained along the shin using the groove on the side with a clamping mechanism. According to the mechanical design, the KFE (Knee flexion-extension) axis to the contact point is 105 mm. Elements of the C-Claw: A) Shin, B) C-Claw Base, C) Cable Canal, D) Tactile Button, E) Rubber, and F) C-Claw Tip.

sense the contact. It is designed in the same geometric form as Part-A to ensure they have a strong grip on each other's surfaces. This helps in achieving a favorable level of friction between them. Part-D is the electronic element and Part-E is the rubber that gives the flexibility to contact with the tactile button without causing damage during the operation. Part-F makes contact with the ground and can move freely inside Part-B. Figure 4 illustrates the working principle of the C-Claw mechanism, which consists of magnets for disengaging from the tactile button. The advantage of magnets instead of linear springs is that they occupy less volume than springs. Also, they do not need any mechanical element to prevent buckling like springs during operation.

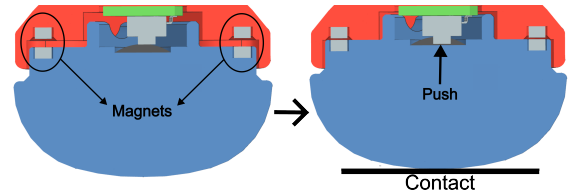


Fig. 4. Cross-section of the C-Claw mechanism: when it engages with the edge of the obstacle, the mechanism activates the tactile button; when it disengages, it turns back to the initial position with the help of magnets that are embedded inside.

To assess the performance of the contact sensing functionality of the C-Claw, we conducted an experiment to identify the minimum activation force for different angles of the force vector. In this experiment, the C-Claw was attached to a Kinova Gen3 manipulator arm and was brought into contact with a force-to-torque sensor, which was fixed to the

workbench. This setup, shown in Fig. 5, was designed to perform multiple contact interactions in a standard way for different contact angles. According to the results presented in Fig. 6, the minimum force for detecting the contacts increases when the C-Claw contact angle becomes more horizontal. As a result, there is no detection of contact beyond the angle of 65° . Hence, the C-Claw's mechanical constraint for contact detection is between -65° to 65° .

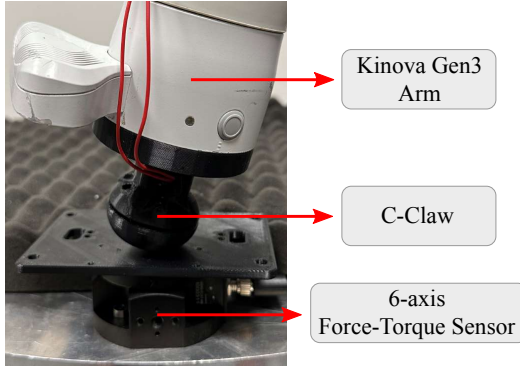


Fig. 5. Experimental setup with a Kinova Gen3 arm to perform multiple contact interactions and assess the sensitivity of the C-Claw contact sensor.

III. EXPLOITING THE C-CLAW ACTIVATION INTO A LOCOMOTION CONTROLLER

In this section, we describe how the acquired contact information from the C-Claw contact sensor can be interpreted and inserted into a locomotion control algorithm to plan the leg motion. To do so, we make use of our Reactive Control Framework (RCF) [22], which is a basic locomotion framework structure equipped with modules to plan the footholds, generate the leg swing motion, and stabilize the body motion. The robot stabilization is done by a whole-body controller that receives as input a desired stabilizing body wrench and computes desired joint torques. Our whole-body controller takes into account constraints regarding joint torque limits, physical consistencies, unilateral ground reaction forces, and surface friction limits [23]. For the sake of space, some details of the motion generation and control are not described in this paper to give focus on the C-Claw feedback into the locomotion framework.

We take a minimalist approach and make use of RCF without any visual feedback, i.e. for blind locomotion, to highlight the intrinsic benefits of the proposed mechanism. During blind locomotion, the foot positions during leg support phases are the main feedback information to plan the next footprint and generate posture references. To do so, the foot contact positions are used to estimate an average plane that can represent the terrain inclination, as well as estimate a relative height of the robot w.r.t. the terrain. When the C-Claw mechanism detects its engagement with the obstacle, the reasoning about the current contact location of a leg, location of potential supporting surfaces, terrain inclination, and robot height can be interpreted in a different manner. The next sub-sections describe how the C-Claw activation (C-Claw contact detection) affects such reasoning.

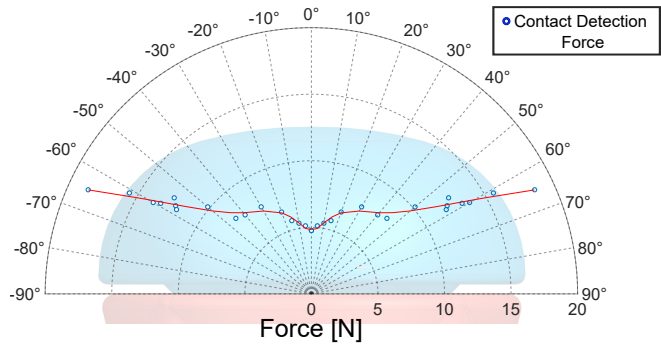


Fig. 6. Polar chart describing the forces needed to detect a C-Claw contact with a surface at different orientations. The blue shaded area represents a planar projection of the C-Claw tip shape. The blue dots represent the force measurements and the red line a corresponding fitted curve.

A. Estimation of leg contact locations

The first and most important information obtained from the C-Claw is the detection of a more accurate contact location during the interaction of the lower-leg with the environment. Given that many robots acquire a foot contact condition through joint torques, and not from foot contact sensors, such information is inconsistent in case of contacts that happen at the lower-leg (i.e. the robot's shin) and not at the foot. Such inconsistent feedback jeopardizes the whole-body controller that ends up producing joint torques, and so the ground reaction forces, according to the wrong leg contact Jacobians. This may result in the robot getting stuck when traversing obstacles [24]. For this matter, a C-Claw activation informs the control framework of a more accurate leg contact Jacobian to be considered for the generation of the joint torques of its corresponding leg, improving the robot's stabilization.

B. Generation of robot attitude and height references

As previously introduced, a very common approach to estimating the relative height between the robot and the terrain is to consider the foot positions during the support phase. In a similar manner, an average terrain inclination is computed to generate references for the robot's attitude. In general, such an attitude is set to be parallel to the estimated terrain inclination. Figure 7 illustrates the robot height and terrain inclination with dashed and solid red lines, respectively. Such estimations are less representative when descending high obstacles and are likely to be dangerous since both of them increase the chances that the robot experiences a long free fall. With the C-Claw mechanism, this problem is mitigated by detecting when the contact is happening only at the C-Claw (reading its activation signal) and no contact is experienced by the foot. In this situation, the strategy we take is to assume the terrain surface is located underneath the foot by a Δ distance (inside the leg workspace). This adjusted foot position is then used for the estimation of the robot height and the terrain inclination, illustrated in Fig. 7 by dashed and solid blue lines, respectively.

The height and attitude references generated from the C-Claw activation adds safety to the locomotion since they have

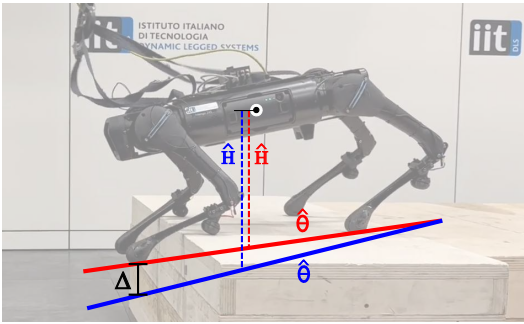


Fig. 7. Estimation of robot height \hat{H} (vertical dashed lines) and terrain pitch inclination $\hat{\theta}$ (solid lines) on irregular surfaces. Red lines indicate estimations considering that contacts can only happen at foot level (a common approach), and blue lines when considering contact events at the foot and C-Claw (proposed feedback). The parameter Δ is the position offset in the vertical direction for the foot when its corresponding C-Claw is active.

an overall effect of reducing the clearance between the floor and the robot's head, which reduces the chances of long and uncontrolled free falls.

IV. EXPERIMENTAL RESULTS

To validate the C-Claw as a mechanism that can increase the capabilities of a quadruped robot for obstacle negotiation, and to demonstrate how the feedback from an active C-Claw enhances the locomotion robustness and safety, we performed various experiments comprising two different scenarios and three robot configurations. As experimental scenarios, we consider high-obstacle descending and locomotion on stairs. As robot configurations, we consider an Aliengo robot without the C-Claw (nominal configuration), an Aliengo equipped with a passive C-Claw (no contact feedback), and an Aliengo equipped with an active C-Claw (with contact feedback). For the experiments, the locomotion control framework commands the robot to execute a static crawling gait at 0.1 m/s. The scenes of all the experimental evaluation reported in this section are included in the accompanying video.

A. Hardware setup

The locomotion control framework runs on an external operator's PC connected via Ethernet cable to the Aliengo robot, which receives all the control commands through ROS Control. The signals from the active C-Claws are acquired by an Arduino Uno mounted on the robot and such information is sent to the operator's PC through ROS messages.

B. Descending from high stair-like obstacles

In this scenario, the robot is required to descend an obstacle that is 40cm in height (equivalent to 80% of its maximum leg length). On top of the obstacle, the robot walks with a relative body height of 30 cm, which leads to an initial head-to-floor clearance of 70cm (as depicted in Fig. 1). Figure 8 shows a sequence of screenshots of the experiments with the three robot configurations: without C-Claw (top row); with passive C-Claw (middle row); and with active C-Claw (bottom row).

Following the top row in Fig. 8 one can see that, without the C-Claw, the Aliengo robot experiences an uncontrolled free fall that leads to a complete loss of stability after touching down with the front legs. From the sequence in the middle, that regards the passive C-Claw, such free fall is substantially reduced so that the robot is able to stabilize the descending. This first difference in performance represents a clear increment in the locomotion robustness. Moreover, by just having a passive C-Claw, the robot is able to reduce the amount of kinetic energy it needs to dissipate with the front legs during the descent, demanding less joint effort. Lastly, for the scene sequence depicted in the bottom row, the robot is equipped with active C-Claws and implements the feedback strategies described in Sec. III. In this case, the robot can detect when the C-Claw makes contact with the obstacle and, therefore, can compute better pose estimates and references. Most importantly, it can produce more consistent ground reaction forces. Overall, it is able to perform a controlled and smooth descending without experiencing dangerous contact interactions.

C. Stair-climbing

The stair-climbing scenario was chosen to assess the C-Claw for being a scenario that imposes challenges for most of the quadruped robots, as mentioned in Sec. I. The risk of locomotion failures during stair climbing depends on the leg kinematic configuration of the robot and the walk direction in which the robot is commanded to stair climb (i.e., walking forward or backward). The risks also increase the lower the ratio between the robot's leg length over the value of each stair's rise. The Spot robot, for example, chooses a preferable walk direction to climb up and down the stairs to avoid undesired leg shin collisions. The same problem and solution would apply to all robots that have both front and hind legs with the same knee-bent orientation (e.g., Aliengo). Therefore, in this experimental evaluation, we command the three Aliengo configurations to climb up a short stair (of 28 cm run and 16 cm rise), by walking backward. This way, we expose the robot to a well-known locomotion challenge to assess how the C-Claw can add to the robot's capabilities in such a scenario. The results of the three experiments are presented through a sequence of screenshots depicted in Fig. 9. The stair's rise corresponds to 32% of Aliengo's leg length.

Observing the screenshot sequence of Fig. 9 on the top, the Aliengo configuration without the C-Claw is not able to climb up the stairs due to the above-mentioned problem of lower-leg collisions with the stairs' edges. When Aliengo is equipped with a passive C-Claw, it is partially able to climb, experiencing many unsuccessful stepping attempts. The performance with a passive C-Claw is clearly superior to without it but the locomotion cannot be considered robust. With a passive C-Claw, the robot does not perform the motion in a fully controlled manner due to the inconsistency between the true leg contact locations and the ones considered by the whole-body controller. When equipped with the active C-Claw, the robot is able to smoothly walk backward as the proposed mechanism naturally engages with the stairs

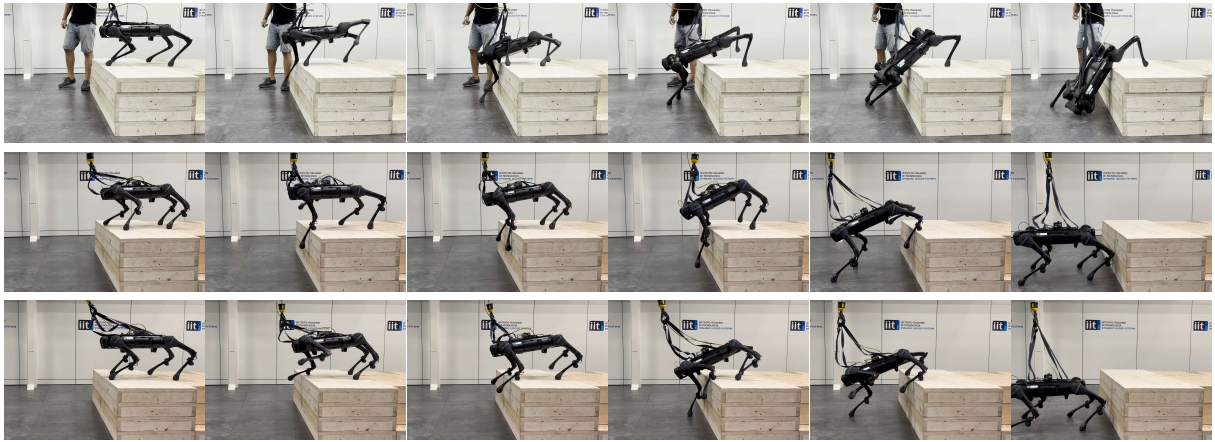


Fig. 8. From left to right, sequence of screenshots during high-obstacle descending for the three robot configurations: without C-Claw (top); with passive C-Claw (middle); and with active C-Claw (bottom). For the experiment with active C-Claw, we considered $\Delta = -0.1$ m (see Sec. III-B).

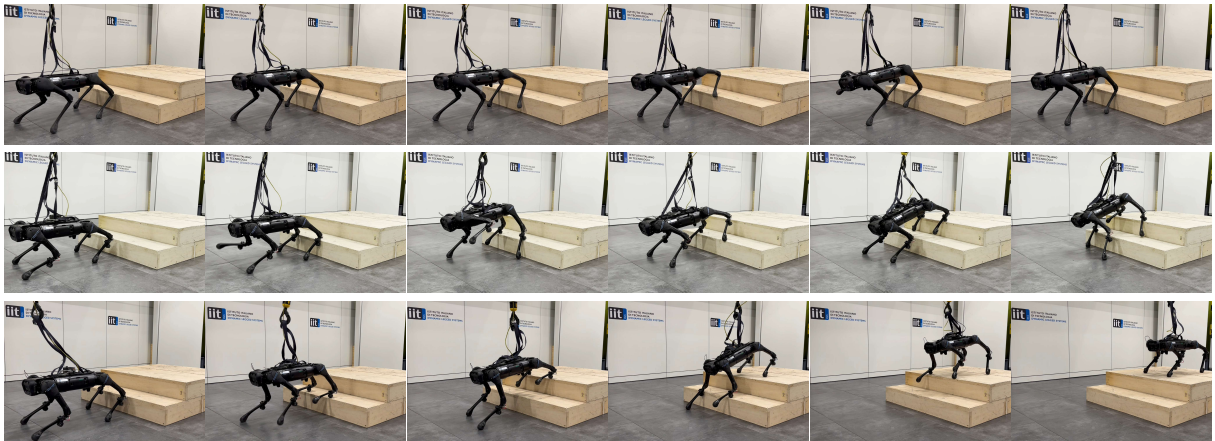


Fig. 9. From left to right, sequence of screenshots during stair-climbing walking backward for the three robot configurations: without C-Claw (top); with passive C-Claw (middle); and with active C-Claw (bottom). The steps are 28cm long and 16cm in height.

and provides feedback to update the leg contact locations. The performance difference between robot configurations can also be noticed by the position reached by each robot in the last screenshot. We observe that the robot does not need to choose a preferable walking direction to climb stairs when endowed with the active mechanism. In the accompanying video, we show that the robot preserves natural walking when also climbing down the stairs with the active C-Claw.

V. CONCLUSIONS

In this paper, we introduced a leg mechanism called C-Claw that enhances the robot's capabilities when negotiating stairs and high obstacles. The proposed mechanism increases the locomotion safety for such obstacle negotiation by allowing the robot to have a more controlled movement and keep the joint torque demands closer to nominal values. We have demonstrated that the robot, with the C-Claw, is able to easily stair-climb up and down when walking forward and backward, overcoming well-known limitations imposed by the leg configuration. Furthermore, the robot is able to descend from a 40 cm high obstacle (equivalent to 80% of the robot's maximum leg length). In both scenarios, the robot

performs the locomotion in a controlled manner under static and quasi-static stability.

All the experiments were performed using blind locomotion and a simple motion generator and controller as a minimalist approach to demonstrate the benefits of the C-Claw. Therefore, it is important to highlight that the gained advantages are intrinsic to the principles behind the mechanism and independent of the implemented locomotion controller. Thus, combining the C-Claw with state-of-the-art locomotion algorithms that also consider visual feedback can only increase the effectiveness of motion planning.

Due to the wide possibilities to combine the C-Claw with other locomotion controllers, future work will focus on extending the mechanism design to other robots and exploiting it inside state-of-the-art model-based and reinforcement learning control algorithms.

ACKNOWLEDGMENT

We would like to thank Matteo Villa, Franco Seguezzo, Marco Marchitto and Juan David Gamba Camacho for their support with the mechanics, electronics, software, and hardware testing setup, respectively.

REFERENCES

- [1] B. Dynamics, "Spot autonomous navigation," https://www.youtube.com/watch?v=Ve9kWX_KXus, May 2018.
- [2] M. Hutter, C. Gehring, A. Lauber, F. Gunther, C. D. Bellicoso, V. Tsounis, P. Fankhauser, R. Diethelm, S. Bachmann, M. Blösch *et al.*, "Anymal-toward legged robots for harsh environments," *Advanced Robotics*, vol. 31, no. 17, pp. 918–931, 2017.
- [3] "Unitree's aliengo robot," <https://www.unitree.com/en/aliengo/>, accessed: 08/05/2023.
- [4] G. Bledt, M. J. Powell, B. Katz, J. Di Carlo, P. M. Wensing, and S. Kim, "Mit cheetah 3: Design and control of a robust, dynamic quadruped robot," in *2018 IEEE/RSJ International Conference on Intelligent Robots and Systems (IROS)*. IEEE, 2018, pp. 2245–2252.
- [5] S. Fahmi, V. Barasoul, D. Esteban, O. Villarreal, and C. Semini, "Vital: Vision-based terrain-aware locomotion for legged robots," *IEEE Transactions on Robotics*, vol. 39, no. 2, pp. 885–904, 2022.
- [6] V. Barasoul, S. Emre, and C. Semini, "Stair-climbing charts: on the optimal body height for quadruped robots to walk on stairs," in *Accepted for International Conference on Climbing and Walking Robots (CLAWAR)*, 2023.
- [7] P. Fankhauser and M. Hutter, "Anymal: a unique quadruped robot conquering harsh environments," *Research Features*, vol. 126, pp. 54–57, 2018.
- [8] P. Fankhauser, M. Bjelonic, C. D. Bellicoso, T. Miki, and M. Hutter, "Robust rough-terrain locomotion with a quadrupedal robot," in *2018 IEEE International Conference on Robotics and Automation (ICRA)*. IEEE, 2018, pp. 5761–5768.
- [9] L. Ye, Y. Wang, X. Wang, H. Liu, and B. Liang, "Optimized static gait for quadruped robots walking on stairs," in *2021 IEEE 17th International Conference on Automation Science and Engineering (CASE)*. IEEE, 2021, pp. 921–927.
- [10] Q. Liang, B. Li, Y. Xu, L. Hou, and X. Rong, "Vision-based dynamic gait stair climbing algorithm for quadruped robot," in *2022 IEEE International Conference on Robotics and Biomimetics (ROBIO)*. IEEE, 2022, pp. 1390–1395.
- [11] S. Qi, W. Lin, Z. Hong, H. Chen, and W. Zhang, "Perceptive autonomous stair climbing for quadrupedal robots," in *2021 IEEE/RSJ International Conference on Intelligent Robots and Systems (IROS)*. IEEE, 2021, pp. 2313–2320.
- [12] A. Kumar, Z. Fu, D. Pathak, and J. Malik, "Rma: Rapid motor adaptation for legged robots," in *Robotics: Science and Systems*, 2021.
- [13] J. Lee, J. Hwangbo, L. Wellhausen, V. Koltun, and M. Hutter, "Learning quadrupedal locomotion over challenging terrain," *Science Robotics*, vol. 5, no. 47, p. eabc5986, 2020. [Online]. Available: <https://www.science.org/doi/abs/10.1126/scirobotics.abc5986>
- [14] A. Agarwal, A. Kumar, J. Malik, and D. Pathak, "Legged locomotion in challenging terrains using egocentric vision," in *6th Annual Conference on Robot Learning*, 2022. [Online]. Available: <https://openreview.net/forum?id=Re3NjSwf0WF>
- [15] D. Hoeller, N. Rudin, D. Sako, and M. Hutter, "Anymal parkour: Learning agile navigation for quadrupedal robots," *arXiv preprint arXiv:2306.14874*, 2023.
- [16] D. Kim, D. Carballo, J. Di Carlo, B. Katz, G. Bledt, B. Lim, and S. Kim, "Vision aided dynamic exploration of unstructured terrain with a small-scale quadruped robot," in *2020 IEEE International Conference on Robotics and Automation (ICRA)*, 2020, pp. 2464–2470.
- [17] Q. Nguyen, M. J. Powell, B. Katz, J. D. Carlo, and S. Kim, "Optimized jumping on the mit cheetah 3 robot," in *2019 International Conference on Robotics and Automation (ICRA)*, 2019, pp. 7448–7454.
- [18] N. Rudin, D. Hoeller, M. Bjelonic, and M. Hutter, "Advanced skills by learning locomotion and local navigation end-to-end," in *2022 IEEE/RSJ International Conference on Intelligent Robots and Systems (IROS)*, 2022, pp. 2497–2503.
- [19] H.-W. Park, P. M. Wensing, and S. Kim, "Jumping over obstacles with mit cheetah 2," *Robotics and Autonomous Systems*, vol. 136, p. 103703, 2021. [Online]. Available: <https://www.sciencedirect.com/science/article/pii/S0921889020305431>
- [20] P. Kanajar, D. G. Caldwell, and P. Kormushev, "Climbing over large obstacles with a humanoid robot via multi-contact motion planning," in *2017 26th IEEE International Symposium on Robot and Human Interactive Communication (RO-MAN)*, 2017, pp. 1202–1209.
- [21] H. E. Evans and A. De Lahunta, *Guide to the Dissection of the Dog-E-Book*. Elsevier Health Sciences, 2016.
- [22] V. Barasoul, J. Buchli, C. Semini, M. Frigerio, E. R. De Pieri, and D. G. Caldwell, "A reactive controller framework for quadrupedal locomotion on challenging terrain," in *IEEE International Conference on Robotics and Automation (ICRA)*, 5 2013, pp. 2554–2561.
- [23] M. Focchi, R. Orsolino, M. Camurri, V. Barasoul, C. Mastalli, D. G. Caldwell, and C. Semini, *Heuristic Planning for Rough Terrain Locomotion in Presence of External Disturbances and Variable Perception Quality*. Springer International Publishing, 2020, pp. 165–209.
- [24] V. Barasoul, G. Fink, M. Focchi, D. G. Caldwell, and C. Semini, "On the detection and localization of shin collisions and reactive actions in quadruped robots," in *International Conference on Climbing and Walking Robots (CLAWAR)*, Oct 2019.